No Universal Urban Form Heat Relationship: Contrasting Thermal Controls in African Cities

Authors:
Liangyu Xian a, *
Maoran Sun b

Affiliations:
a School of Design and Art, Beijing Institute of Technology, Beijing 102488, China
b Sustainable Design Group, University of Cambridge, CB2 1PX, Cambridge, UK

* Corresponding author
E-mail address: 3220242773@bit.edu.cn
ORCID (Liangyu Xian): https://orcid.org/0009-0001-3006-3884
ORCID (Maoran Sun): https://orcid.org/0000-0001-7218-3553

This manuscript is currently under review at *Landscape and Urban Planning*.
This is an unpeer-reviewed preprint submitted to EarthArXiv.

Abstract

Rapid urbanization and climate change have intensified urban heat island effects. Tropical African cities face particularly high heat vulnerability, yet they remain underrepresented in urban thermal research. Existing research often assumes universal morphology temperature relationships, lacking cross city comparative evidence and spatially rigorous nonlinear attribution in African contexts. This study examines daytime land surface temperature (LST) associations with 11 multi dimensional urban morphological indicators in Lagos and Nairobi, using a nested 2 km spatial block cross validation framework coupled with XGBoost and SHAP analysis. Results reveal markedly city specific regulation patterns. In compact, densely built Lagos, population density dominates, while vegetation morphology is the primary control in fragmented, greener Nairobi. Nonlinear threshold effects are detected for building density in Lagos and vegetation height in Nairobi, and single shot imagery systematically amplifies factor contributions compared with multi temporal composites. These findings demonstrate that urban morphology temperature relationships are not uniform across African cities, supporting context specific rather than unified heat mitigation planning.

Keywords: Land surface temperature; Urban morphology; Urban heat island; XGBoost; SHAP; African cities

1 Introduction

Rapid urbanization and global climate change have intensified urban heat island effects worldwide (Zhou et al., 2004; Georgescu et al., 2014), making land surface temperature (LST) regulation a critical priority for climate adaptive urban planning. This challenge is particularly acute in tropical African cities, where urban expansion is occurring at unprecedented rates (UN-Habitat, 2016; Fox, 2012) and heat vulnerability remains high (Rohat et al., 2021; Kunda et al., 2024). Despite this urgency, African cities remain underrepresented in urban thermal research compared with their counterparts in Europe, North America, and East Asia (Ngie et al., 2014; Gyimah, 2023; Li et al., 2022). Given this research gap, understanding the contributors to urban thermal environments in these rapidly changing contexts is essential for safeguarding public health and livability.

A common implicit assumption in existing urban thermal research is that the same urban form produces comparable thermal responses across cities (Arnfield, 2003). Under this assumption, more built up areas are universally warmer and more vegetation is universally cooler (Li et al., 2011; Zhao et al., 2023; Yang et al., 2019), providing a seemingly transferable basis for heat mitigation planning. Studies modeling the spatial relations between urban morphology, land surface temperature, and energy demand further reinforce this expectation of consistent morphology temperature coupling (Chen et al., 2020). However, growing evidence suggests that morphology temperature relationships may be strongly city specific (Lemoine-Rodríguez et al., 2022), particularly across diverse urban development contexts in Africa. Whether the same morphological indicator exerts comparable thermal effects across distinct urban contexts remains largely untested, especially in sub Saharan Africa where urban thermal studies remain scarce (Simwanda et al., 2021).

Existing studies have established statistical associations between LST and urban morphological indicators such as building density (Zhao et al., 2023; Han, 2023; Yuan et al., 2021), impervious surface fraction, and vegetation cover (Li et al., 2011; Weng et al., 2004; Peng et al., 2012). Machine learning approaches have further quantified the relative contributions of urban fabric components, with building coverage ratio and vegetation index identified as dominant factors in dense urban contexts (Okumus and Terzi, 2021). Nevertheless, the majority of this research has focused on landscape composition and coverage metrics, while structural attributes of urban form such as building height, vegetation volume, and the competition between built and ecological spaces have received less attention. More fundamentally, cross city comparative studies remain scarce, particularly for rapidly urbanizing regions in sub Saharan Africa. Existing multi city assessments have largely concentrated on European or Asian contexts (Marando et al., 2022), where diverse urban development trajectories may produce fundamentally different morphology temperature coupling mechanisms.

From a methodological perspective, recent machine learning applications in urban thermal modelling have commonly relied on random cross validation, which can introduce spatial data leakage and overestimate model generalisation performance when applied to spatially autocorrelated remote sensing data (Meyer et al., 2019; Roberts et al., 2017). From a data perspective, early urban thermal studies predominantly relied on local survey data and field measurements, with research concentrated in cities of the Global North (Ching et al., 2018). However, the increasing availability of globally covered open data products such as satellite derived LST, building footprints, canopy height, and population grids has created new opportunities for scalable and transferable urban thermal research in data scarce regions of the Global South (Middel et al., 2022). Open multi source datasets have already enabled local climate zone mapping and heat risk assessment in rapidly urbanizing contexts (Zhou et al., 2021). Consequently, there is a lack of spatially rigorous, nonlinear attribution analyses that leverage open multi dimensional urban morphological data to compare city specific thermal regulation mechanisms across tropical African cities.

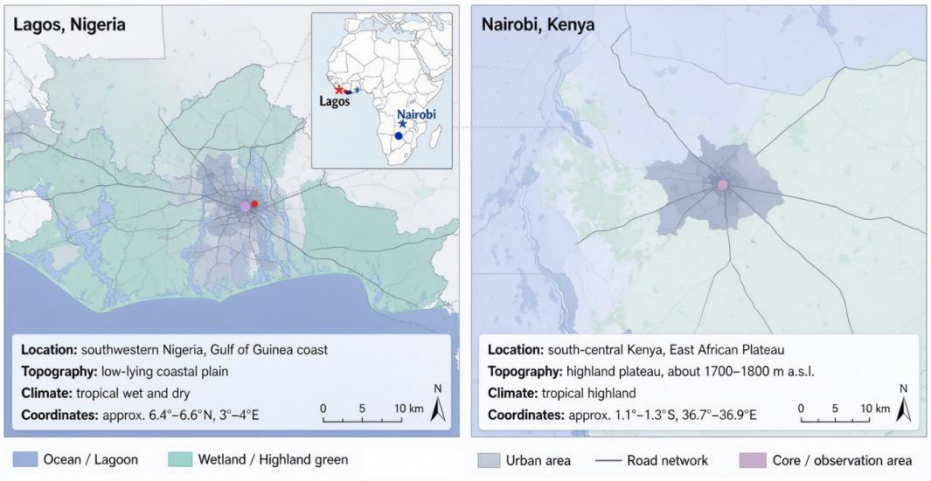
To address these gaps, this study conducts a cross city comparative analysis of two rapidly urbanizing tropical African cities, Lagos and Nairobi, to examine whether and how associations between urban morphology and daytime LST differ across distinct urban development contexts. Multi source open geospatial datasets are integrated to construct 11 morphological indicators grouped into four categories: building morphology, vegetation morphology, integrated building vegetation morphology, and population density. A nested spatial block cross validation framework coupled with an XGBoost regression model is employed to capture nonlinear associations while preventing spatial information leakage, and SHAP analysis is applied to quantify the contribution of individual indicators. The research design further includes a comparison between single shot instantaneous and multi temporal composite ECOSTRESS LST inputs as a sensitivity analysis, enabling an assessment of both city specific thermal regulation patterns and the robustness of attribution results.

This study addresses the following research questions: (1) How do multi dimensional urban morphological indicators nonlinearly associate with daytime land surface temperature in tropical African cities? (2) To what extent do the dominant contributors to LST variation differ between Lagos and Nairobi, and what do these differences reveal about city specific coupling mechanisms? (3) How does the choice between single shot instantaneous imagery and multi temporal composite products affect the magnitude and interpretation of factor attribution? By answering these questions, this study aims to provide quantitative evidence for climate adaptive urban planning in rapidly urbanizing tropical regions.

2 Materials and methods

2.1 Study Area

Two fast growing African cities, Lagos (Nigeria) and Nairobi (Kenya), were selected as study cases in this work. Lagos is located on the Atlantic coast of south western Nigeria (approximately 6.4° N, 3.4° E), representing a densely populated coastal megacity. It features a tropical wet and dry climate, with a rainy season from April to October and a dry season period spanning November to March. Constrained by satellite data availability, dry season observations from November 2024 to February 2025 were adopted for thermal analysis in this study.



By contrast, Nairobi lies in the Kenyan highlands at around 1700 m above sea level (approximately 1.3° S, 36.8° E). Owing to its high elevation equatorial climate, Nairobi exhibits mild overall temperatures, with February March as its warmest dry season phase before the onset of long rains.

Both cities are undergoing rapid urban sprawl and informal settlement expansion, which brings prominent urban heat island effects and complex three dimensional built environment patterns. The present research focuses on the urban cores of Lagos and Nairobi, rather than full administrative boundaries, to investigate the coupling relationships between urban morphology and land surface temperature.

2.2 Data

In this section, we describe the datasets used in this study. The primary data sources include Land Surface Temperature, building footprints, building height, digital elevation, vetegation height, remote sensing and sociodemographic data. The same data sources and downloading procedures were applied consistently across both cities to ensure comparability.

LST data were derived from the ECOSTRESS ECO2LSTE Level 2 thermal product (Hook et al. 2019) with a native spatial resolution of approximately 70 m. To capture typical hot season thermal conditions, daytime observations were selected for the two study cities during their dry and hottest seasons. Specifically, LST observations for Nairobi were acquired in February - March 2025, while data for Lagos covered November 2024–February 2025. All valid LST pixels were spatially aggregated to the unified 100 m analytical grid using zonal mean statistics, forming consistent thermal variables for subsequent urban thermal analysis.

Building footprints were obtained from the Microsoft GlobalML Building Footprints dataset(Microsoft, 2023), which provides vector polygons covering the study area. The footprint data serve as the geometric basis for computing building morphology metrics. For Nairobi, 379,478 building polygons were identified; for Lagos, 1,151,803 building polygons were extracted using the same procedure.

Building height information was sourced from the GlobalBuildingAtlas (Zhu et al., 2025), which provides global building height estimates at 3 m resolution. The identical datasets and download

workflows were applied for both cities.

Vegetation morphology was characterized using the ETH Global Canopy Height dataset at 10 m resolution. For Nairobi, tiles S02E036 and S02E037 were used; for Lagos, tile N06E02 was downloaded following the same procedure.

Additionally, Pervious Surface Fraction (PSF) was derived from Landsat 8 OLI Collection 2 Level 2 surface reflectance imagery (USGS, 2020) at 30 m resolution. For Nairobi, Path 168, Row 061 was used; for Lagos, the corresponding Path/Row covering the city was selected using the identical download and processing workflow. NDBI (Normalized Difference Built up Index) was also calculated for impervious surface characterization. Two composite indices were derived to capture the integrated effects of building and vegetation morphology, as detailed in Section 2.3.1.

Population Density (PD) was obtained from the GHSL GHS POP dataset (Schiavina et al., 2023) at 100 m resolution, expressed as persons per hectare. The same dataset was applied for both Nairobi and Lagos. Additionally, SRTM 1 Arc Second Global digital elevation data (EROS Center, 2019) at 30 m resolution were incorporated to account for topographic context and terrain effects on LST.

After the above mentioned processing steps, a complete dataset containing the 11 derived indicators and the LST target variable was compiled for subsequent analytical workflows.

2.3 methods

As described in Section 2.2, multi source datasets covering the study area were collected to build a multi dimensional urban spatial morphology indicator system, with population density adopted to represent anthropogenic heat release. With the requested data, we further constructed multi dimensional morphological metrics and a 100 m analytical grid, and generates composite daytime LST data to support subsequent analysis. To mitigate spatial leakage risks in geospatial modelling, a nested 2 km spatial block cross validation scheme is adopted. Pearson correlation is applied for preliminary linear exploration, followed by a spatially constrained XGBoost SHAP workflow to capture nonlinear interactions and quantify factor contributions. This framework disentangles linear non linear coupling relationships between urban form and thermal environment.

2.3.1 Analytical Grid and Construction of the Urban Spatial Morphology Indicator System

To conduct spatial quantitative analysis, we established a 100 m grid system to consistently align LST and each morphological indicator within grid cells. The 100 m grid is a commonly used scale for coupling urban thermal environment and morphology (Sun et al., 2023), as it accurately captures block scale temperature variations while maintaining computational efficiency. Considering the varying native resolutions of multi source geospatial datasets and the built environment features of the two African cities, we selected 100 m as the suitable analytical scale.

It worth noticing that not all downloaded data are at the geospatial resolution of 100m. To account for this, a rigorous vector raster clipping workflow was applied for grid generation under the UTM coordinate system. All multi source geospatial datasets were resampled and aggregated onto this

unified 100 m analytical grid. Edge cell indicators were normalized by real land area to eliminate statistical bias from irregular administrative borders. Polygon fragments smaller than 1 m² were excluded during processing.

This study selected 11 quantitative indicators for correlation analysis against land surface temperature. The metrics were classified into four categories: building morphology (BM), vegetation morphology (VM), building vegetation integrated morphology (BVIM), and population density (PD). Referring to existing research on urban thermal environments and urban spatial morphology (He et al., 2023; Masoudi and Tan, 2019; Ma et al., 2016), the four group indicators jointly describe built up features, vegetation related traits, coupled building vegetation spatial characteristics and human activity intensity.

The building morphology metrics include building density, floor area ratio, average height, building volume and pervious surface fraction. The building morphology indicators are based on building density (BD), floor area ratio (FAR), average building height (ABH), building volume (BV), and pervious surface fraction (PSF). The detailed definition for each indicator is followed:

- Building Density (BD): $\mathrm{BD} = \frac{A_{build}}{A_{cell}}$
- Average Building Height (ABH): $\mathrm{ABH} = \frac{1}{n}\sum_{i=1}^{n} h_i$
- Building Volume (BV): $\mathrm{BV} = \sum_{i=1}^{n} (A_i \times h_i)$
- Floor Area Ratio (FAR): $\mathrm{FAR} = \frac{\mathrm{BV}}{3 \times A_{cell}}$

The vegetation morphology metrics include vegetation mean height (VMH), vegetation volume (VV), and vegetation height variance (VHV):

- Vegetation Mean Height (VMH): $\mathrm{VMH} = \frac{1}{m}\sum_{j=1}^{m} H_j$
- Vegetation Volume (VV): $\mathrm{VV} = \sum_{j=1}^{m} (H_j \times a_{pixel})$
- Vegetation Height Variance (VHV): $\mathrm{VHV} = \frac{1}{m}\sum_{j=1}^{m} (H_j - \mathrm{VMH})^2$

Indicators for building morphology include building density (BD), floor area ratio (FAR), average building height (ABH), building volume (BV) and pervious surface fraction (PSF). Vegetation morphology metrics consist of vegetation mean height (VMH), vegetation volume (VV), and vegetation height variance (VHV).

Besides representing building and vegetation morphology respectively, we also constructed building vegetation integrated morphology indicators to capture the coupled effects of built and ecological spaces. Two normalized difference indices were derived:

- Normalized Difference Vegetation to Building Volume Ratio (NDVR): $\mathrm{NDVR} = \frac{\mathrm{BV}-\mathrm{VV}}{\mathrm{BV}+\mathrm{VV}}$
- Normalized Difference Height Ratio (NDHR): $\mathrm{NDHR} = \frac{\mathrm{ABH}-\mathrm{VMH}}{\mathrm{ABH}+\mathrm{VMH}}$

Scaled between −1 and 1, they reflect the vertical volume competition between built up and ecological space and support comparative analysis across cities.

Population Density (PD) was included as the fourth indicator category to represent anthropogenic activity intensity and associated heat emission. Sourced from the GHSL GHS-POP dataset at 100

m resolution and expressed as persons per hectare, PD captures variations in human occupancy across urban neighbourhoods, complementing the physically based morphological indicators.

2.3.2 Daytime Land Surface Temperature Retrieval and Composite

This study employed the ECOSTRESS ECOv002 Level 2 Temperature (L2T) georeferenced land surface temperature product for daytime urban thermal environment analysis. A unified data preprocessing workflow was implemented using Python and the rasterio library. The original UTC timestamps of the imagery were converted to West Africa local time (UTC+1), and daytime clear sky observations between 10:00 and 18:00 were selected as valid data sources, which covered the main daylight heating period after local sunrise and before sunset across the West African study region. Adjacent tile images acquired within an interval of less than 2 minutes were grouped as a single satellite overpass. Based on MGRS tile completeness, complete overpass data covering the study area were screened to ensure spatial continuity and temporal validity of the time series observations.

Each LST image underwent raster preprocessing: reprojection and resampling were performed according to the target coordinate system, spatial resolution, and boundary extent of the study area, using mean resampling to accommodate the continuous variable nature of land surface temperature. Temperature values were converted from Kelvin to degrees Celsius using the formula ($T(^\circ C) = T(K) - 273.15$). A reasonable temperature range of 250 – 350 K was set to exclude abnormal values. This threshold covers the physically plausible land surface temperature scope for tropical urban areas: values below 250 K mainly represent cloud contaminated noise, while pixels exceeding 350 K are regarded as sensor induced extreme outliers impossible for natural ground surfaces; any invalid pixels with outliers or out of range values were uniformly assigned as null (NaN).

Based on the unified 100 m analytical grid established in Section 2.3.1, coordinate system and grid parameter verification were conducted to eliminate spatial registration biases, ensuring uniform analytical units across multi temporal images. Preprocessed single scene LST data were matched to the unified grid. To reduce instantaneous errors from cloud coverage and atmospheric interference, we adopted a pixel based multi temporal average composite approach. Each grid cell required no fewer than two valid observations before calculation. This process ultimately yielded a standardized, high quality time series LST dataset, providing reliable foundational data for subsequent analysis of the coupling between urban morphology and the thermal environment.

2.3.3 Spatial Dependence and Cross Validation Strategy Design

As a typical spatially continuous variable, land surface temperature (LST) generally exhibits significant positive spatial autocorrelation, meaning that geographically adjacent grid cells tend to share similar thermal characteristics (Anselin, 1995). This spatial dependence poses a potential threat to the reliability of model evaluation: under the conventional random K fold cross validation framework, spatially proximate samples can easily be split between training and validation sets by chance, allowing the model to indirectly access spatial information from the validation set during training, a phenomenon known as spatial data leakage. As a result, the generalisation error is underestimated, and the model's predictive performance in independent geographic regions is

overestimated (Brenning, 2012; Roberts et al., 2017). To address this issue, spatial block cross validation strategies are widely recognised as an effective means of preventing spatial information leakage (Meyer et al., 2019; Ploton et al., 2020).

This study adopts a nested 2 km spatial block cross validation strategy. The procedure is as follows: we divided the study area into non overlapping rectangular spatial blocks with a side length of 2,000 m. All grid cells within a given block were treated as a single group unit. During cross validation splits, entire spatial blocks were assigned to a fold, ensuring that no block was shared between the training and validation sets i.e., the spatial distance between any training grid and any validation grid was at least 2 km. This threshold was chosen based on two considerations: first, a 2 km buffer is sufficient to break most of the spatial autocorrelation range typical of urban thermal environments (Varentsov et al., 2021; Xiao-qin, 2007); second, this scale ensures adequate sample sizes within each fold to support robust model training and evaluation (Schratz et al., 2019; Meyer et al., 2019). Through this design, the interference of spatial dependence on model performance assessment was largely eliminated.

The model architecture employed a nested double loop structure, with its methodological rationale lying in decoupling hyperparameter optimisation from generalisation error estimation under a spatially independent framework (Cawley and Talbot, 2010):

(1) Outer loop (5 fold spatial partitioning): used to evaluate the true generalisation capability of the model. The dataset was divided into five subsets based on spatial blocks. In each iteration, one subset served as the validation set and the remaining four as the training set, and the predicted values for the validation samples (out of fold predictions, OOF) were recorded for each iteration. The 5 fold design balances training sample size (80%) and validation sample size (20%), consistent with common practice in spatial block cross validation (Schratz et al., 2019).

Inner loop (4 fold spatial partitioning): performed exclusively on the current outer training set. It further split the data into four spatial block subsets and executed a grid search over hyperparameters (including n_estimators, max_depth, and learning_rate). This inner loop was independent of the outer validation set, ensuring that hyperparameter selection was based solely on the training data and avoiding information leakage during tuning (Vabalas et al., 2019). The optimal hyperparameter combination, as determined by inner spatial block cross validation performance on the current outer training set, was then used to predict the outer validation set.

(2) Missing value handling strategy: all preprocessing procedures, median based missing value imputation included, are processed separately for each training subset. This workflow guarantees that statistical parameters for imputation are calculated only from the current training dataset instead of the full sample dataset, which avoids information leakage from the validation set during data preprocessing (Kuhn and Johnson, 2013).

2.3.4 Preliminary Feature Screening and Correlation Analysis

In this study, we used the Pearson correlation coefficient to perform bivariate linear correlation analysis between each morphological indicator and LST, aiming to reveal the direction and strength of their statistical dependence. The Pearson correlation coefficient (r) measures the

degree of linear covariation between two continuous variables, defined as the ratio of their covariance to the product of their standard deviations:

$$r = \frac{\sum_{i=1}^{n}(x_i - \bar{x})(y_i - \bar{y})}{\sqrt{\sum_{i=1}^{n}(x_i - \bar{x})^2}\sqrt{\sum_{i=1}^{n}(y_i - \bar{y})^2}}$$

where x_i and y_i represent the morphological indicator value and LST value for the i-th grid cell, respectively, and $\bar{x}$ and $\bar{y}$ are their sample means. The value of r ranges from -1 to 1; the sign indicates the direction of association, and the absolute value reflects the strength of the linear relationship.

The Pearson correlation analysis provides a preliminary basis for factor screening prior to the subsequent XGBoost nonlinear modeling, and the directional patterns identified can serve as a reference benchmark for validating the plausibility of the nonlinear model results.

2.3.5 Nonlinear Attribution Model and Interpretability Analysis

Urban land surface temperature is regulated by the nonlinear and interactive effects of built environment, three dimensional vegetation structure, and population agglomeration (Alavipanah et al., 2018; Zhou et al., 2017). Traditional linear statistical models cannot adequately capture the complex interactions among variables, whereas conventional machine learning approaches with random K fold cross validation neglect the intrinsic spatial autocorrelation of remote sensing raster data. The overlapping information of neighbouring grid samples leads to spatial data leakage, overestimates model generalisation accuracy, and thus fails to reliably reveal the driving mechanisms of regional thermal environments. To overcome these limitations, this study constructed a spatial block cross validation framework coupled with an XGBoost regression model.

Specifically, the XGBoost regression model was trained under the spatial block cross validation framework illustrated in Section 2.3.3. All preprocessing procedures including median based missing value filling are executed independently inside each training subset to avoid preprocessing induced information leakage. After model training, SHAP interpretation was adopted to quantify the nonlinear driving effects of urban morphological factors.

The native feature importance provided by XGBoost merely counts variable weights based on split frequency, which cannot distinguish between positive (warming) and negative (cooling) driving directions, nor quantify the spatial heterogeneity of factor contributions across cities and temporal observations, resulting in insufficient statistical interpretability. Therefore, we introduced SHAP (SHapley Additive exPlanations) theory for posterior attribution analysis. Based on the optimally trained spatially constrained XGBoost model, we computed the mean absolute SHAP value (mean_abs_SHAP) for each morphological indicator to quantify its global contribution to LST variation. By comparing the modelling results across two cities, multi temporal composite

imagery, and clear sky single scene imagery (four scenarios in total), we identified regional differences and temporal sensitivity in the dominant thermal drivers.

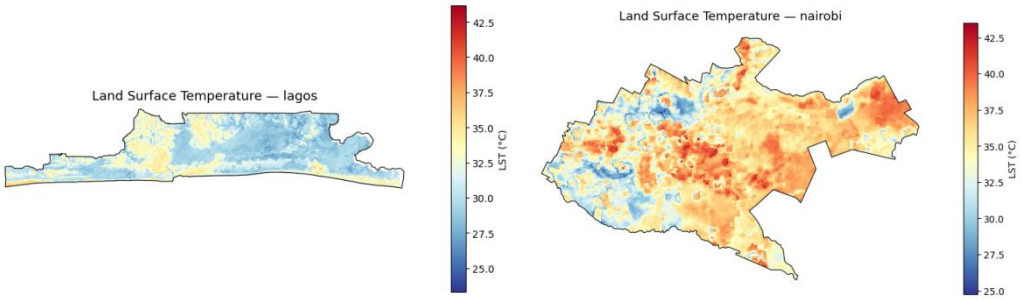
This nested spatially constrained XGBoost SHAP framework constitutes a complete analytical chain “spatial bias correction + nonlinear fitting + multi scenario quantitative attribution”. On the one hand, it corrects the misuse of spatial information in conventional machine learning via spatial block cross validation, ensuring rigorous and reliable simulation results. On the other hand, it quantitatively clarifies the differentiated regulatory effects of three dimensional vertical vegetation structure, built up patterns, and population density on surface temperature in tropical cities. The results empirically support the theoretical hypothesis that building morphology, vegetation morphology and building vegetation integrated morphology indicators jointly shape urban thermal differentiation, providing quantitative evidence for heat island mitigation planning in tropical African cities.

3 result

3.1 Spatial Distribution Characteristics of Land Surface Temperature

3.1.1 Spatial and Numerical Distribution of LST in Lagos

Lagos exhibited a spatial pattern dominated by low temperatures across most of the city, with only scattered patches of high temperatures locally. This pattern is closely associated with Lagos's coastal geographical setting: extensive water bodies and coastal wetlands penetrate the urban interior, and sea breezes continuously moderate the near surface air temperature, effectively suppressing the development of continuous urban heat islands. The frequency histogram of 100 m grid LST revealed a bimodal distribution in Lagos, corresponding respectively to cool areas such as water bodies, green spaces, and low density residential zones, and to built up residential areas. The number of grid cells with temperatures above 35 °C dropped sharply, with extremely high temperature samples accounting for a very low proportion, indicating a relatively mild overall thermal environment.



3.1.2 Spatial and Numerical Distribution of LST in Nairobi

Compared with Lagos, Nairobi exhibited significantly higher overall LST and more pronounced spatial differentiation between cool and warm areas. Spatially, the city was dominated by warm orange yellow and reddish brown tones, with extensive contiguous high temperature zones widely distributed across the central and northeastern core urban areas. Only a few scattered patches (in the western part of the city and around small green spaces and water bodies) appeared as cool blue areas, indicating a marked spatial agglomeration of the urban heat island. Nairobi, located on an inland plateau without marine cooling effects, experiences dense urban expansion and fragmented green spaces, which promote continuous heat accumulation and result in large contiguous high

temperature zones. The LST histogram for Nairobi showed an approximately normal unimodal distribution, with the vast majority of grid cells falling within the 32–38 °C range; overall, the city exhibited higher mean LST and greater temperature dispersion.

3.2 Linear Correlation Analysis Between Four Category Urban Indicators and LST

Pearson coefficient comparative analysis was performed on two tropical African cities (Lagos and Nairobi), to explore the correlation between land surface temperature and four groups of indicators: building morphology, vegetation morphology, building vegetation integrated morphology and population density.

For building morphology indicators, positive correlations with LST were observed in both cities, consistent with the basic urban heat island theory. Building density (BD) showed the strongest positive association with LST among all morphological indicators, with correlation coefficients of 0.601 in Lagos and 0.171 in Nairobi. Floor area ratio (FAR), representing horizontal urban development intensity, also exhibited positive correlations (0.437 in Lagos, 0.155 in Nairobi). Average building height (ABH) and building volume (BV) capture heat and solar radiation via street canyon effects, attaining moderate positive correlations in Lagos (0.479 and 0.437, respectively), whereas in Nairobi these two metrics showed barely detectable linear relationships (0.001 and 0.155, respectively). The inter city disparity reflects differences in urban texture: large scale connected low rise informal settlements in Lagos create extensive impervious ground and hinder air circulation, associated with sustained heat accumulation, whereas Nairobi's scattered construction land interspersed with green patches greatly weakens the warming influence of horizontal built up layouts.

Table 3.2a. Pearson correlation coefficients between LST and building morphology / population density indicators.

Indicator	Full name	Lagos	Nairobi	|Diff.|	Direction
BD	Building Density	0.601	0.171	0.430	Positive (warming)
FAR	Floor Area Ratio	0.437	0.155	0.282	Positive (warming)
ABH	Average Building Height	0.479	0.001	0.478	Positive (warming)
BV	Building Volume	0.437	0.155	0.282	Positive (warming)
PD	Population Density	0.428	0.131	0.297	Positive (warming)

Note: |Diff.| = absolute difference between Lagos and Nairobi coefficients. All building morphology and population density indicators show positive associations with LST in both cities.

Vegetation morphology parameters displayed distinct cooling associations in both cities. Vegetation mean height (VMH) and vegetation volume (VV) served as stable negative correlates of LST. Nairobi possessed larger continuous green land patches and delivered stronger shading and evapotranspiration cooling, with correlation coefficients of −0.577 and −0.608, whose absolute values exceeded Lagos' −0.341 and −0.454. Vegetation height variance (VHV) showed no notable linear association with LST in either city (−0.010 in Lagos, −0.092 in Nairobi), indicating that total vegetation biomass, rather than vertical structural heterogeneity, determines cooling potential.

Table 3.2b. Pearson correlation coefficients between LST and vegetation / integrated morphology indicators.

Indicator	Full name	Lagos	Nairobi	|Diff.|	Direction
VMH	Vegetation Mean Height	−0.341	−0.577	0.236	Negative (cooling)
VV	Vegetation Volume	−0.454	−0.608	0.154	Negative (cooling)
VHV	Vegetation Height Variance	−0.010	−0.092	0.082	Weak / negligible
NDVR	NDVR (Vegetation-to-Building Vol. Ratio)	0.349	0.346	0.003	Positive (warming)
NDHR	Norm. Diff. Height Ratio	0.331	0.352	0.021	Positive (warming)
PSF	Pervious Surface Fraction	0.232	0.010	0.222	Weak positive

Note: |Diff.| = absolute difference between Lagos and Nairobi coefficients. Vegetation morphology indicators show negative (cooling) associations, while integrated morphology indicators are mostly positive.

For building vegetation integrated morphology indicators, the normalized difference building to vegetation volume ratio (NDVR) and normalized difference building to vegetation height ratio (NDHR), which measure the volumetric disparity between built and ecological spaces, were significantly positively correlated with LST in both cities. The coefficients were comparable between Lagos (0.349 and 0.331) and Nairobi (0.346 and 0.352). Higher index values indicate that building volume far exceeds the carrying capacity of vegetation, such that the cooling effect of vegetation cannot offset the heat accumulation from impervious surfaces and canyon trapping, associated with elevated LST. The pervious surface fraction (PSF) presented weak positive correlations with LST in both cities (0.232 in Lagos, 0.010 in Nairobi), failing to produce detectable cooling effects. Under year round hot tropical climate conditions, small sized and fragmented permeable patches cannot form stable cool islands via evapotranspiration.

Population density (PD) was positively associated with surface warming in both research cities. Lagos recorded a correlation coefficient of 0.428, noticeably higher than Nairobi's 0.131. This gap reflects stronger anthropogenic heat emissions associated with the densely distributed population within Lagos.

Overall, built up expansion is associated with warming while vegetation retention is associated with cooling, a common feature of both tropical cities. The linear regulatory effect of built patterns on LST is stronger in Lagos, whereas vegetation cooling predominates in Nairobi, fundamentally attributable to differences in urban development patterns and planning systems between the two cities.

3.3 Nonlinear Associations Between Urban Metrics and LST Based on Interpretable XGBoost SHAP

3.3.1 Generalisation Performance Evaluation of the Spatial block Cross Validation Model

Land surface temperature raster data shows strong spatial autocorrelation. Meanwhile, systematic disparities in model prediction accuracy were detected between Lagos and Nairobi. Overall, urban areas with compact built up structures and homogeneous impervious surfaces achieved higher model accuracy, and remote sensing data with less spatiotemporal noise further improved explanatory performance. For the multi temporal daytime dataset of Lagos, the 5 fold mean coefficient of determination was $R^2 = 0.6121 \pm 0.0309$, with negligible fluctuation across folds; the pooled out of fold R^2 reached 0.630 with an RMSE of 1.208°C. The optimal accuracy range from inner tuning converged stably, and hyperparameter values were highly consistent, indicating optimal model convergence and spatial generalisation. For Nairobi, the multi temporal

composite daytime data, affected by daily variations in water vapour and atmospheric conditions combined with high landscape heterogeneity, yielded a lower baseline accuracy: the 5 fold mean $R^2 = 0.4442 \pm 0.1142$, with OOF $R^2 = 0.4903$ and notable cross fold variation. However, when replacing the composite with a single scene instantaneous image acquired under optimal clear sky conditions, thus eliminating temporal environmental noise, the model accuracy rebounded substantially, with a 5 fold mean $R^2 = 0.5895 \pm 0.0623$ and $R^2 = 0.6180$, approaching the performance level observed for Lagos.

These results confirm that higher spatial compactness of urban built up areas leads to more homogeneous thermal patterns and stronger explanatory power of urban morphological factors for the thermal environment. Conversely, thermal heterogeneity induced by interspersed green spaces and temporal scales significantly influence urban thermal conditions.

3.3.2 Nonlinear Contribution Ranking of Morphological Factors Using SHAP

Building upon the reliable predictive accuracy achieved by the XGBoost models, with pooled OOF $R^2 = 0.621$ and RMSE = 1.22°C for the multi temporal composite model in Lagos, and $R^2 = 0.490$ and RMSE = 1.41°C for the corresponding model in Nairobi, we further quantified the contribution strength of each morphological indicator to LST predictions using the mean absolute SHAP value (mean_abs_SHAP).

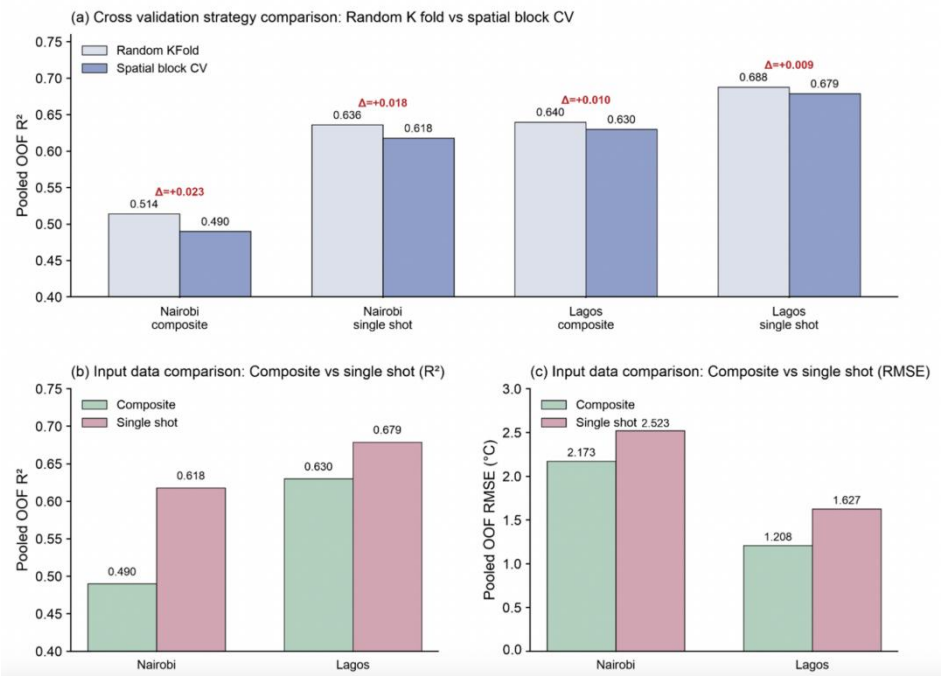
In the two Lagos model scenarios, population density (PD) consistently emerged as the dominant controlling factor with the highest contribution. Under the multi temporal composite model, the mean absolute SHAP value of PD reached 0.8223, and further increased to 1.3668 in the clear sky single scene model, with its contribution advantage substantially surpassing all other indicators. Vegetation mean height (VMH, 0.3337/0.5039) and vegetation volume (VV, 0.2899/0.2467) ranked second and third, respectively, indicating that the cooling effect of three dimensional vegetation structure was secondary. Contributions from built environment and coupling indices (building density (BD) and NDVR) were generally low, with most indicators having SHAP values below 0.30. The predominant role of PD in Lagos stems from the sharp urban rural spatial gradient, where differential population aggregation, coupled with built up expansion and changes in impervious surface fraction, collectively drive LST spatial differentiation. It should be noted that this result reflects statistical association rather than direct heat generation from population.

In the two Nairobi model scenarios, three dimensional vegetation indicators dominated overwhelmingly. In the multi temporal composite model, VV (0.8829) and VMH (0.8538) exhibited mean absolute SHAP values far ahead of all other variables. Under the clear sky single scene scenario, VMH contribution surged to 1.8612, becoming the top driver across the entire domain, while VV (0.6994) remained in second place. Although PD still showed some explanatory power (0.4336 and 0.5126 for the two scenarios), its contribution intensity was considerably lower than in Lagos. Contributions from two dimensional built form indicators (ABH, FAR, and BD) were generally weak, with SHAP values all below 0.23.

4 discussion

4.1 Model reliability and city specific factor contribution patterns

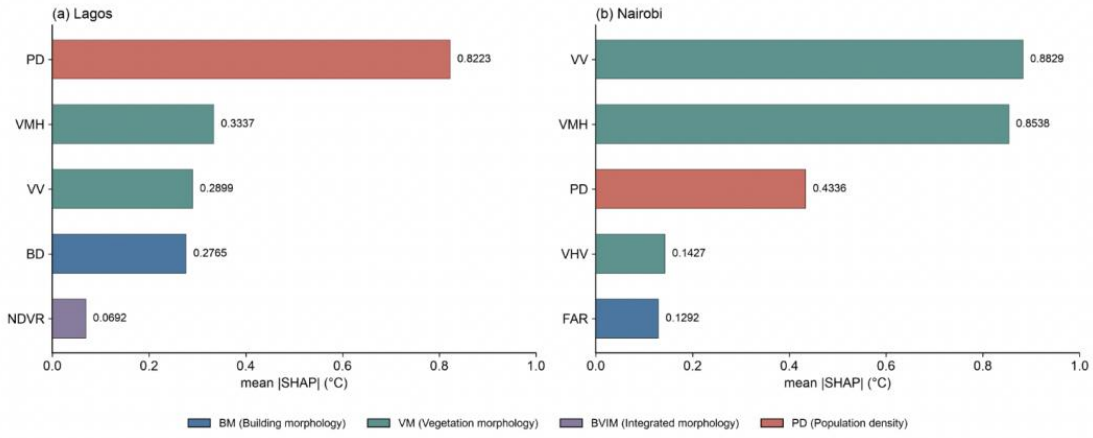
To ensure the reliability of model performance assessment, we first compared random K fold cross validation with spatial block cross validation. The clearest methodological finding is that 99.999% of random fold test cells belonged to 2 km neighborhoods also represented in training, compared with 0% under spatial block cross validation. Across all four experimental groups, random cross validation consistently yielded higher R squared values, with 95 percent block bootstrap intervals not covering zero, confirming statistically significant overestimation caused by spatial data leakage. The R squared difference reached 0.023 for the Nairobi composite dataset and 0.010 for the Lagos composite dataset, indicating that fragmented urban landscapes are more vulnerable to leakage effects. Therefore, all subsequent analyses are based on spatial block cross validation metrics.



As a sensitivity analysis, we further compared single shot instantaneous and multi temporal composite ECOSTRESS inputs. Single shot cloud free imagery yielded higher pooled out of fold R squared for both cities (Nairobi: 0.490 to 0.618; Lagos: 0.630 to 0.679) but larger absolute RMSE (Nairobi: 2.173 to 2.523 °C; Lagos: 1.208 to 1.627 °C), reflecting the larger spatial heterogeneity of instantaneous LST fields (single shot SD: 4.08 °C in Nairobi, 2.87 °C in Lagos; composite SD: 3.04 °C and 1.99 °C respectively). Single shot imagery also systematically amplified SHAP contribution magnitudes (Nairobi VMH: 0.8538 to 1.8612 °C; Lagos PD: 0.8223 to 1.3668 °C). Given that composite products better represent average dry season thermal conditions and produce more conservative attribution results, the composite dataset was adopted as the primary input for factor attribution analysis.

Based on the spatial block cross validation model trained on the composite dataset, SHAP analysis revealed markedly different factor contribution patterns between the two cities. For Lagos, population density (PD) was the dominant predictor with a mean absolute SHAP value of 0.8223 °C, followed by vegetation mean height (VMH, 0.3337 °C), vegetation volume (VV, 0.2899 °C), and building density (BD, 0.2765 °C). For Nairobi, vegetation volume (VV,

0.8829 °C) and vegetation mean height (VMH, 0.8538 °C) were the two leading contributors, followed by population density (PD, 0.4336 °C), whereas building morphology indicators such as floor area ratio (FAR, 0.1292 °C) made relatively limited contributions. This inter city divergence in dominant contributors indicates that the coupling mechanisms between urban morphology and surface temperature are not uniform across cities, motivating the detailed comparative analysis in the following section.



4.2 Contrasting thermal regulation mechanisms across Lagos and Nairobi

The most striking finding of this study is that the same set of urban morphological indicators produces fundamentally different thermal regulation patterns in Lagos and Nairobi. In Lagos, population density and built environment intensity exert the strongest control on surface temperature, whereas in Nairobi, vegetation morphological structure is the primary regulator. This divergence challenges the assumption of universal morphology temperature relationships and suggests that heat mitigation strategies must be city specific.

In Lagos, the dominance of population density (SHAP = 0.8223 °C) reflects the city's compact, densely built urban form. Spontaneous dense settlements occupy a large proportion of the urban core, and continuous impervious surfaces amplify anthropogenic heat accumulation. High population density corresponds to intensified human activities and heat emission, which becomes one of the leading warming contributors in this city. Building morphology indicators, particularly building density (0.2765 °C), also play substantial roles, as large scale connected low rise informal settlements create extensive impervious ground and hinder air circulation, contributing to sustained heat accumulation. Vegetation morphology variables still produce observable cooling benefits, but their overall contribution strength is surpassed by built environment and population factors.

In Nairobi, by contrast, vegetation morphology indicators dominate thermal regulation. Vegetation volume (0.8829 °C) and vegetation mean height (0.8538 °C) far exceed all other variables in contribution strength. Fragmented green patches are widely interspersed within built up areas, and their shading and evapotranspiration cooling effects consistently show prominent influences. Even though building density can raise local surface temperature, the scattered construction layout in Nairobi weakens its overall warming magnitude. Population density presents a relatively limited influence (0.4336 °C), which may be related to the city's relatively planned urban expansion pattern and more balanced spatial distribution of residents. Building morphology indicators such

as FAR (0.1292 °C) make only marginal contributions, as wider building gaps and scattered high rise constructions produce weak street canyon effects.

The nonlinear response patterns further underscore these mechanistic differences. For Lagos, building density produces growing warming effects once it exceeds a certain threshold: dense low rise self built constructions block horizontal air flow and trap near surface heat, further aggravating thermal risks. For Nairobi, the cooling efficiency of vegetation indicators gradually rises with increasing vegetation height until reaching a relatively stable saturation level, suggesting that tall, continuous vegetation patches are particularly effective cooling sources in this fragmented green built mosaic. The building vegetation integrated morphology indicators also show heterogeneous performance: in Lagos, rapid built land expansion and vertical space occupation by buildings significantly weaken the cooling function of underlying green elements, whereas in Nairobi, the interleaving pattern of buildings and vegetation mitigates such competitive pressure and maintains relatively good thermal regulation capacity of urban greenspace.

The inconsistent contribution ranks derived from SHAP and linear Pearson correlation analysis confirm the existence of complex nonlinear interactions between urban indicators and surface thermal environment. While Pearson correlations show broadly expected directions (built up indicators positive, vegetation indicators negative), SHAP reveals very different dominant mechanisms between the two cities. These differences imply that heat mitigation strategies cannot adopt a unified standard for all tropical African cities. Local landscape characteristics and urban development modes must be fully considered when formulating morphological based cooling measures, as the same intervention may produce markedly different thermal outcomes in Lagos versus Nairobi.

4.3 Planning implications, limitations and future perspectives

The divergent thermal regulation mechanisms identified in Lagos and Nairobi carry important implications for climate adaptive urban planning. Most fundamentally, this study demonstrates that the same urban form does not produce comparable thermal responses across African cities: population density and built intensity dominate in compact, densely built Lagos, while vegetation morphological structure is the primary control in fragmented, greener Nairobi. Therefore, transferable urban heat mitigation cannot rely on universal morphology rules, and planning strategies must be tailored to each city's specific development context.

For Lagos, a coastal metropolis dominated by contiguous low rise informal built environments, thermal accumulation is strongly associated with continuous impervious surfaces and intense competition between buildings and limited green space. Planning should prioritize the systematic governance of sprawling informal residential areas, optimize the vertical configuration of built and ecological elements, and promote targeted vertical greening interventions to alleviate heat accumulation in dense homogeneous urban textures. For Nairobi, a highland city characterized by fragmented green built mosaics, scattered vegetation patches serve as critical cooling sources. Urban management should strictly protect fragmented green infrastructures and implement early thermal risk prevention in newly emerging high population density zones to avoid excessive anthropogenic thermal disturbance. These city specific findings provide useful references for climate adaptive urban planning in rapidly urbanizing cities across sub Saharan tropical regions,

while cautioning against direct transfer of mitigation strategies between cities with distinct urban forms.

Several limitations should be acknowledged. First, this analysis focused on dry season daytime LST from ECOSTRESS, without covering nighttime or wet season conditions. Diurnal and seasonal thermal variations may reshape morphological thermal relationships, and future work could incorporate multi seasonal and day night continuous LST datasets. Second, cross city comparability is constrained by differing data acquisition windows (10:00–17:00 EAT for Nairobi, 10:00–18:00 WAT for Lagos) and different target temperature variances; reported R^2 and RMSE should not be interpreted as a cross city performance ranking. For Lagos, the absence of companion quality control bands meant that cloud and noise screening relied exclusively on a 10–60 °C physical threshold, and a QC layer sensitivity analysis would be desirable. Third, terrain variables were not included, which may be particularly relevant for highland Nairobi, and input layers from different acquisition epochs may not perfectly represent concurrent urban conditions. Fourth, fine scale microclimate factors such as wind field and near surface air temperature were not incorporated; subsequent research could combine microclimate monitoring to disentangle interactions between urban form and local atmospheric factors. Fifth, the unified 100 m grid cannot fully capture micro scale thermal heterogeneity within block level units; finer grids or local climate zone classification may help in follow up work.

Finally, the scope of inference must be clearly bounded. SHAP values quantify model derived predictive associations rather than causal effects, especially given correlations among morphological predictors. The spatial block cross validation estimates transfer to held out 2 km neighborhoods within the same observed city, but do not establish transferability across cities, seasons, sensors, or years. Model performance should therefore be described as spatial interpolation to geographically held out blocks rather than forecasting of future thermal conditions. Residual noise from satellite products and spatial mismatch among multi source datasets may also introduce minor bias. Despite these limitations, the core finding that urban morphology temperature relationships are strongly city specific provides a robust foundation for context aware heat mitigation planning in tropical African cities.

5 conclusion

Rapid urbanization and global climate change have intensified urban heat island effects worldwide, posing significant threats to public health and urban livability, particularly in rapidly growing tropical African cities. Existing research has long assumed that the same urban form produces comparable thermal responses across cities, yet cross city comparative evidence remains scarce, especially in sub Saharan Africa. This study addresses this gap through a spatially rigorous nonlinear attribution analysis comparing Lagos and Nairobi.

Three key findings emerge. First, spatial block cross validation consistently yielded lower R squared values than random K fold cross validation, confirming significant spatial data leakage and establishing spatial block cross validation as the more reliable evaluation framework. Single shot instantaneous imagery produced higher R squared but larger RMSE and amplified SHAP contributions compared with composite products, confirming that composite inputs provide more

conservative attribution results. Second, the dominant thermal contributors differ fundamentally between cities: population density leads in compact, densely built Lagos (mean absolute SHAP = 0.8223 °C), while vegetation volume and vegetation mean height dominate in fragmented, greener Nairobi (0.8829 and 0.8538 °C respectively). Third, nonlinear threshold effects further distinguish the two cities: building density shows accelerating warming beyond a threshold in Lagos, whereas vegetation cooling efficiency increases with height until saturation in Nairobi.

These findings demonstrate that urban morphology temperature relationships are strongly city specific, challenging the assumption of universal thermal response patterns. For climate adaptive planning, Lagos should prioritize governance of dense informal settlements and vertical greening, while Nairobi should protect fragmented green infrastructures and prevent thermal risk in emerging high density zones. Despite limitations including dry season daytime only coverage and bounded spatial transferability, this study provides robust evidence for context aware heat mitigation in rapidly urbanizing tropical African cities.

References

Alavipanah, S., Schreyer, J., Haase, D., Lakes, T., Qureshi, S. (2018). The effect of multi-dimensional indicators on urban thermal conditions. Journal of Cleaner Production, 192, 117–126.

Anselin, L. (1995). Local indicators of spatial association—LISA. Geographical Analysis, 27(2), 93–115.

Arnfield, A.J. (2003). Two decades of urban climate research: a review of turbulence, exchanges of energy and water, and the urban heat island. International Journal of Climatology, 23(1), 1–26.

Brenning, A. (2012). Spatial cross-validation and bootstrap for the assessment of rule-based models in landslide susceptibility mapping. In Proceedings of the 10th International Symposium on Spatial Accuracy Assessment in Natural Resources and Environmental Sciences, 155–160.

Yang, J., Jin, S., Xiao, X., Jin, C., Xia, J.C., Li, X., Wang, S. (2019). Local climate zone ventilation and urban land surface temperatures: Towards a performance-based and wind-sensitive planning proposal in megacities. Sustainable Cities and Society, 47, 101487. https://doi.org/10.1016/j.scs.2019.101487

Okumus, D.E., Terzi, F. (2021). Evaluating the role of urban fabric on surface urban heat island: The case of Istanbul. Sustainable Cities and Society, 73, 103128. https://doi.org/10.1016/j.scs.2021.103128

Cawley, G.C., Talbot, N.L.C. (2010). On over-fitting in model selection and subsequent selection bias in performance evaluation. Journal of Machine Learning Research, 11, 2079–2107.

Ching, J., et al. (2018). Cities and Climate Change: an Urbanization Imperative. Bulletin of the American Meteorological Society, 99(10), 2107–2111.

Elvidge, C.D., Baugh, K.E., Kihn, E.A., Kroehl, H.W., Davis, E.R. (1997). Relation between satellite observed visible-near infrared emissions, population, economic activity and electric power consumption. International Journal of Remote Sensing, 18(6), 1373–1379.

EROS Center (2019). SRTM 1 Arc-Second Global. NASA Shuttle Radar Topography Mission. U.S. Geological Survey.

Fox, J. (2012). Africa's urban transition. Geoforum, 43(3), 429–435.

Gao, S., Chen, Y., Chen, D., He, B., Gong, A., Hou, P., Li, K., Cui, Y. (2024). Urbanization-induced warming amplifies population exposure to compound heatwaves but narrows exposure inequality between global North and South cities. npj Climate and Atmospheric Science, 7, 55.

Georgescu, M., Morefield, P.E., Bierwagen, B.G., Weaver, C.P. (2014). Urban adaptation can roll back warming of emerging megapolitan regions. Proceedings of the National Academy of Sciences, 111(8), 2909–2914.

Zhou, Y., Zhang, G., Jiang, L., Chen, X., Xie, T., Wei, Y., Xu, L., Pan, Z., An, P., Lun, F. (2021). Mapping local climate zones and their associated heat risk issues in Beijing: Based on open data. Sustainable Cities and Society, 74, 103174.

Gyimah, R.R. (2023). The hot zones are cities: Methodological outcomes and synthesis of surface urban heat island effect in Africa. Cogent Social Sciences, 9(1), 2165651.

He, R., Wang, J., Liu, D. (2023). Assessing the impact of urban spatial form on land surface temperature using random forest—Taking Beijing as a case study. Land, 12(2), 437.

Hook, S.J., et al. (2019). In-flight validation of the ECOSTRESS, Landsats 7 and 8 thermal infrared spectral channels. IEEE Transactions on Geoscience and Remote Sensing.

Kuhn, M., Johnson, K. (2013). Applied Predictive Modeling. Springer, New York.

Kunda, J.J., Gosling, S.N., Foody, G.M. (2024). The effects of extreme heat on human health in tropical Africa. International Journal of Biometeorology, 68, 1015–1033.

Lang, N., et al. (2023). High-resolution global canopy height map. Nature Ecology & Evolution, 7(11), 1778–1789.

Marando, F., Heris, M.P., Zulian, G., Udías, A., Mentaschi, L., Chrysoulakis, N., Parastatidis, D., Maes, J. (2022). Urban heat island mitigation by green infrastructure in European Functional Urban Areas. Sustainable Cities and Society, 77, 103564. https://doi.org/10.1016/j.scs.2021.103564

Chen, H.C., Han, Q., De Vries, B. (2020). Modeling the spatial relation between urban morphology, land surface temperature and urban energy demand. Sustainable Cities and Society, 60, 102246.

Lemoine-Rodríguez, R., et al. (2022). Does urban climate follow urban form? Science of the Total Environment, 838, 156475.

Li, J., Song, C., Cao, L., Zhu, Y., Liu, D. (2011). Impacts of landscape structure on surface urban heat islands: A case study of Shanghai, China. Remote Sensing of Environment, 115(12), 3249–3263.

Li, X., Stringer, L.C., Dallimer, M. (2022). The impacts of urbanisation and climate change on the urban thermal environment in Africa. Climate, 10(11), 164.

Ma, Q., Wu, J., He, C. (2016). A hierarchical analysis of the relationship between urban impervious surfaces and land surface temperatures: spatial scale dependence, temporal variations, and bioclimatic modulation. Landscape Ecology, 31, 1139–1153.

Masoudi, M., Tan, P. (2019). Multiscale analysis of the relationship between urban form and land surface temperature. Sustainable Cities and Society, 49, 101587.

Meyer, H., Reudenbach, C., Wöllauer, S., Nauss, T. (2019). Importance of spatial predictor variable selection in machine learning applications – Moving from data reproduction to spatial prediction. Ecological Modelling, 411, 108815.

Middel, A., Nazarian, N., Demuzere, M., Bechtel, B. (2022). Urban climate informatics: An emerging research field. Frontiers in Environmental Science, 10, 867434.

Microsoft (2023). GlobalML Building Footprints. GitHub repository.

Ngie, A., Abutaleb, K., Ahmed, F., Darwish, A., Ahmed, M. (2014). Assessment of urban heat island using satellite remotely sensed imagery: a review. South African Geographical Journal, 96(2), 157–172.

Peng, S., Piao, S., Ciais, P., Friedlingstein, P., Ottlé, C., Viovy, N., Wang, T., Jiao, W. (2012). Surface urban heat island across 419 global big cities. Environmental Science & Technology, 46(2), 696–703.

Ploton, P., et al. (2020). Assessing the accuracy of data-driven models in ecology: A comparison of spatial and non-spatial cross-validation methods. Ecography, 43(12), 1739–1751.

Roberts, D.R., Bahn, V., Ciuti, S., Boyce, M.S., Elith, J., Guillera-Arroita, G., Hauenstein, S., Lahoz-Monfort, J.J., Schröder, B., Thuiller, W., Warton, D.I., Wintle, B.A., Hartig, F., Dormann, C.F. (2017). Cross-validation strategies for data with temporal, spatial, hierarchical, or phylogenetic structure. Ecography, 40(8), 913–929.

Rohat, G., Flacke, J., Dosio, A., Dao, H., Van Maarseveen, M. (2021). Projections of human exposure to dangerous heat in African cities under multiple socioeconomic and climate scenarios. Earth's Future, 9(10), e2021EF002173.

Schiavina, M., et al. (2023). GHS-POP R2023A - GHS population grid multitemporal (1975-2030). European Commission, Joint Research Centre.

Schratz, P., Muenchow, J., Iturritxa, E., Richter, J., Brenning, A. (2019). Hyperparameter tuning and performance assessment of statistical and machine-learning algorithms using spatial data. Ecological Modelling, 406, 109–120.

Simwanda, M., Ranagalage, M., Estoque, R.C., Murayama, Y. (2021). Spatial analysis of surface urban heat islands in four rapidly growing African cities. Remote Sensing, 13(11), 2133.

Sun, Y., Gao, C., Li, J., Wang, R., Liu, J. (2023). Quantifying the effects of urban form on land surface temperature in subtropical high-density urban areas using machine learning. Remote Sensing, 15(3), 789.

UN-Habitat (2016). World Cities Report 2016: Urbanization and Development—Emerging Futures. Nairobi: United Nations Human Settlements Programme.

USGS (2020). Landsat 8 Collection 2 Level-2 Science Products. U.S. Geological Survey.

Vabalas, A., Gowen, E., Poliakoff, E., Casson, A.J. (2019). Machine learning validation methods for quantifying the clinical prognosis of glioblastoma patients. PLOS ONE, 14(11), e0224427.

Varentsov, M., Fenner, D., Meier, F., Samsonov, T., Demuzere, M. (2021). Quantifying local and mesoscale drivers of the urban heat island of Moscow with reference and crowdsourced observations. Frontiers in Environmental Science, 9, 716968.

Weng, Q., Lu, D., Schubring, J. (2004). Estimation of land surface temperature–vegetation abundance relationship for urban heat island studies. Remote Sensing of Environment, 89(4), 467–483.

Xiao-qin, Y. (2007). A spatial analysis of urban heat island and underlying surface using Landsat ETM. Remote Sensing for Land & Resources.

Zhao, J., et al. (2023). Assessing the thermal contributions of urban land cover types. Landscape and Urban Planning, 232, 104669.

Zhou, B., Rybski, D., Kropp, J.P. (2017). The role of city size and urban form in the surface urban heat island. Scientific Reports, 7, 4791.

Zhou, L., Dickinson, R.E., Tian, Y., Fang, J., Li, Q., Kaufmann, R.K., Tucker, C.J., Myneni, R.B. (2004). Evidence for a significant urbanization effect on climate in China. Proceedings of the National Academy of Sciences, 101(26), 9540–9544.

Zhu, X.X., Chen, S., Zhang, F., Shi, Y., Wang, Y. (2025). GlobalBuildingAtlas: An open global and complete dataset of building polygons, heights and LoD1 3D models. Earth System Science Data.